Electroluminescent main-chain copolymers containing phosphorescent benzimidazole-based iridium complexes as copolymerization backbone units or dopants

Wei-Sheng Huang,[a] Ying-Hsien Wu,[b] Hong-Cheu Lin*[a] and Jiann T. Lin*[c]

Received 3rd October 2009, Accepted 5th November 2009
First published as an Advance Article on the web 12th January 2010
DOI: 10.1039/b9py00276f

A series of novel electroluminescent main-chain copolymers containing fluorene-1,4-bis(9-octyl-9*H*-carbarzol-3yl)-2,5-dioctyloxy-benzene (**BCB**) segments and phosphorescent benzimidazole-based iridium (Ir) complexes in the backbones were synthesized by Suzuki coupling reaction. The relative intensity of phosphorescence and fluorescence were affected by the energy transfer and back transfer efficiencies between the polymer backbones and the iridium units as evidenced by solid state PL and EL spectra. PLED devices with a configuration of ITO/PEDOT: PSS (70 nm)/Ir-copolymers (**P3–P10**) or Ir-doped copolymers (**P1–P2** doped with Ir-complex **4**) (60–80 nm)/TPBI (40 nm)/LiF (1 nm)/Al (120 nm) were fabricated, where electroluminescence (EL) efficiencies depended on the chemical constituents and the triplet energies of the copolymers. PLED devices based on Ir-containing copolymer **P8** or copolymer **P2** doped with 5 mol% Ir-complex **4** exhibited white-light emissions with EL properties of $\eta_{ext,max} = 0.93\%$, $\eta_{c,max} = 1.88$ cd A^{-1}, and $L_{max} = 1960$ cd m^{-2} from the former (**P8**), and $\eta_{ext,max} = 4.09\%$, $\eta_{c,max} = 10.94$ cd A^{-1}, and $L_{max} = 4870$ cd m^{-2} from the latter (**P2** doped with Ir-complex **4**), respectively. The CIE coordinates, color-rendering index (CRI) and correlated color temperature (CCT) of the two PLED devices were (0.33, 0.30) at 13 V, 74 and 5966 K for the former, and (0.35, 0.32) at 15 V, 82 and 6147 K for the latter, respectively.

Introduction

Tremendous progress has been made on organic light-emitting diodes (OLEDs) after Tang and Van Slyke's[1] and Burroughes *et al.*'s[2] reports on LEDs consisting of small organic molecules and polymers, respectively. The development of phosphorescent transition metal complexes brought the external quantum efficiency (EQE) of OLEDs to a new milestone, because both singlet and triplet excitons can be harvested and thus an overall 100% internal quantum efficiency is possible.[3] Many metal-based phosphorescent emitters have been developed in the past decade. Among these phosphorescent emitters, iridium,[4] platinum,[5] osmium,[6] and ruthenium[7] complexes have received considerable attention. These complexes were successfully used in polymer light-emitting diodes (PLEDs) and OLEDs which were usually prepared by solution process[8] and vacuum deposition,[9] respectively.

Compared with small molecules, polymers are more suitable for spin-coating or ink-jet techniques which renders flexible substrates and large area displays in conjunction with PLEDs.[10] Nevertheless, the efficiencies of PLEDs fabricated *via* spin-coating are generally lower than those of small molecule-based multi-layer devices fabricated *via* vacuum-deposition. To compensate for the lower efficiencies of PLEDs, iridium complexes were frequently doped into a polymer matrix[11] or directly tethered to the polymer main chains,[12] side chains,[13] or terminals.[14] For example, Gong *et al.* reported a highly efficient yellow-green electrophosphorescent OLED fabricated by doping tris(9,9-dihexyl-2-(pyridinyl-2′)fluorene) iridium(III) ($Ir(DPF)_3$) into poly(*N*-vinylcarbazole) (PVK) blended with the electron-transporting 2-(4-biphenylyl)-5-(4-*tert*-butylphenyl)-1,3,4-oxadiazole (PBD), where an EQE of 10% and luminous efficiency (η_c) of 36 cd A^{-1} were achieved.[11a] Similarly, PVK doped with blue-emitting FIrpic, green-emitting $Ir(ppy)_3$, and red-emitting $(btp)_2Ir(acac)$ complexes exhibited maximum EQE values at 1.3%, 5.1%, and 2.0%, respectively.[11b]

Alternatively, iridium complexes can be tethered to the backbones or side chains of polymers. Among PLEDs, fluorene units and their derivatives have been popularly used because of several advantages: high photoluminescence quantum yield (PLQY); excellent chemical, thermal, and photo stabilities; good solubilities and film-forming properties. Moreover, high-yielding synthetic routes for well-defined and high-molecular-weight polymers are readily available.[15] Chen *et al.* grafted both carbazole and iridium complex moieties to polyfluorenes (PFs) *via* a saturated hydrocarbon spacer tethered at the carbon-9 position of the fluorene unit.[13a] The PLED device containing 1.3 mol% $(btp)_2Ir(acac)$ was reported to have an EQE of 1.59% and a power efficiency (η_p) of 2.8 cd A^{-1} at 7 V with a luminance of 65 cd m^{-2}. A red-emitting 2-(1-naphthalene)pyridine-bicycloiridium/fluorene copolymer developed by Zhen *et al.* was reported to have an EQE of 6.5% at a current density of 38 mA cm^{-2}, and a luminance of 926 cd m^{-2} with an emission peak at 630 nm.[12a]

[a]*Department of Materials Sci. and Eng. National Chiao Tung University, Hsinchu, Taiwan, ROC. E-mail: linhc@cc.nctu.edu.tw; Fax: +8863-5724727; Tel: +8863-5712121 ext. 55305*
[b]*Electro-Optical Engineering and Graduate Institute of Electronics Engineering, National Taiwan University, Taipei, Taiwan, ROC*
[c]*Institute of Chemistry Academia Sinica, Taipei, Taiwan, ROC. E-mail: jtlin@chem.sinica.edu.tw; Fax: +8862-27831237; Tel: +8862-27898522*

Polymers synthesized by Jiang *et al.* had a backbone of fluorene-alt-carbazole with iridium complexes as side groups.[13b] The PLED devices fabricated from the previous polymers had the highest EQE of 4.9%, the luminous efficiency of 4.0 cd A^{-1} with 240 cd m^{-2} at 7.7 V, and the peak emission at 610 nm. Fluorene-alt-carbazole copolymers P(F-alt-Cz)s developed by Zhang *et al.* had cyclometalated iridium fragments ligated to the β-diketone units of the polymer backbones. All fabricated PLED devices were almost free of efficiency decay even at high current density.[12b] Cao and co-workers,[16] Shu and co-workers,[17] and Lee *et al.*[18] demonstrated that white light-emitting OLEDs (WOLEDs) were also possible by incorporation of a blue-emitting fluorene-based copolymer with green and red fluorescent (or phosphorescent) emitters in the backbones and side chains, respectively, where high current efficiencies of 6.1 cd A^{-1} and 4.8 cd A^{-1} were demonstrated correspondingly. It was interesting to note that most of the iridium complexes tethered to the conjugated copolymers were red-emitters.

A series of highly phosphorescent cyclometalated iridium (Ir) complexes containing benzimidazole-based ligands have previously been developed.[19] High performance yellow- and green-emitting OLEDs have been achieved by using these complexes as guest emitters. Later, these Ir-complexes were successfully tethered with dendrons and efficient dendrimer-type LEDs (DLEDs) were fabricated.[20] In view of the aforementioned easy solution-processing of polymers, and handy co-polymerization approach, we decided to extend benzimidazole-based cyclometalated Ir complexes to the polymer systems for possible applications in PLEDs including WOLEDs. For a fair comparison, the iridium units were tethered to the polymers backbones (Ir-copolymers) or doped into the analogous metal-free polymers (Ir-doped copolymers). In this study, we prepared a series of novel PLED copolymers consisting of fluorescent 1,4-bis(9-octyl-9*H*-carbazol-3yl)-2,5-dioctyloxy-benzene (**BCB**), fluorene, and phosphorescent benzimidazole-based Ir-complex units. Analogous metal-free polymers were prepared similarly except that the benzimidazole-based Ir-complex units were omitted. The physical and electroluminescent properties of these PLED copolymers were also investigated.

Results and discussion

Synthesis and characterization

The synthetic routes and chemical structures of the copolymers are shown in Schemes 1–3. The Ir-complexes **3** and **4** were synthesized by following the procedures of their iridium congener, **(pbi)$_2$Ir(acac)**[19] (the structure of **(pbi)$_2$Ir(acac)** is shown Fig. 2(a)). The carbazole-based building block of the polymers, 1,4-bis(6-bromo-9-octyl-9*H*-carbarzol-3yl)-2,5-dioctyloxy-benzene (**BCB-2Br**, **6**), was prepared by two successive steps: (1) Suzuki coupling of 9-octyl-9*H*-carbazol-3-ylboronic acid with 1,4-dibromo-2,5-bis(octyloxy)benzene to provide **BCB**; (2) bromination of **BCB** by using *N*-bromosuccinimide. Two octyloxy substituents were incorporated in **BCB**, where the carbazole segments were introduced to enhance the triplet energy in the polymers. The 2,5-bis(octyloxy)benzene unit in **BCB** was to improve the solubility and film-forming property of the desired copolymers. Copolymerization of monomers

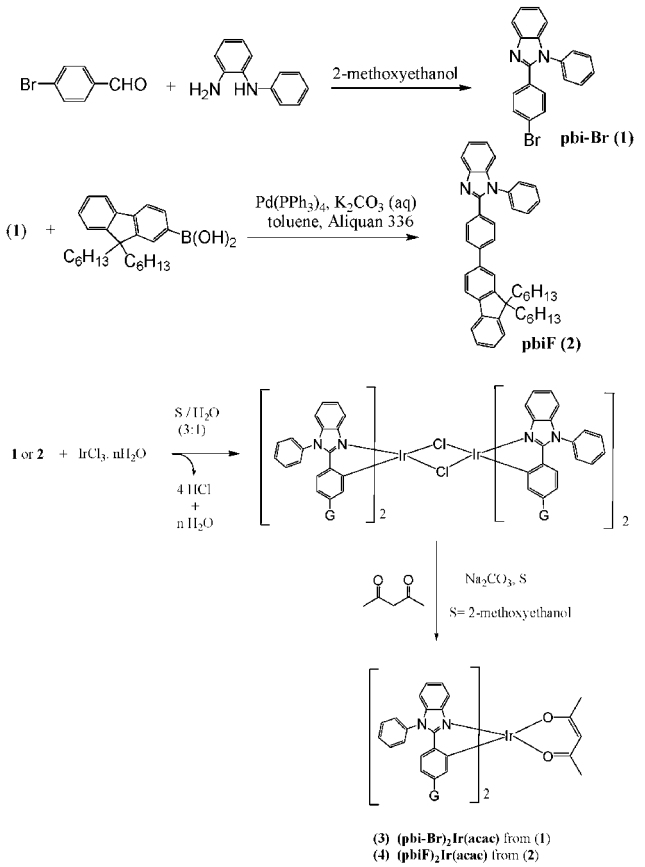

Scheme 1 Synthesis of **bi** ligands (**1** and **2**) and Ir-complexes **3** and **4**.

dibromo-substituted Ir-complex **3**, **BCB-2Br** (**6**), and fluorenes (compounds **7** and **8**) was achieved *via* Suzuki coupling reaction. The feed ratio of the iridium units was controlled at a level of 2, 5, 10, or 20 mol%. All polymers were characterized by ^{1}H NMR spectroscopy, gel permeation chromatography (GPC), and elemental analysis. Actual compositions of the copolymers (characterized by ^{1}H NMR) and the feed ratios of the monomers are listed in Table 1. The number-average molecular weights (M_n) of these copolymers lay in the range of 5000 to 20500 g mol^{-1} with a polydispersity index (PDI) ranging from 1.53 to 2.08.

Electrochemical characterization

The electrochemical behavior of the iridium monomers and all the copolymers were studied by cyclic voltammetric (CV) methods, and the relevant data are listed in Table 2. A quasi-reversible one-electron oxidation wave attributed to the oxidation of iridium(III) was detected at 0.47 and 0.32 V *vs.* Fc/Fc^+ from Ir-complexes **3** and **4**, respectively. However, these oxidation waves were elusive in the Ir-copolymers (**P3–P10**) possibly due to the low contents of Ir-complex **3**. All copolymers (**P1–P10**) in this study exhibited oxidation potentials with the onsets lying in the range of 0.58–0.66 V *vs.* Fc/Fc^+, which can be attributed to the oxidation of the copolymer backbones. The energies of the highest occupied molecular orbitals (HOMOs) in all copolymers were calculated relative to ferrocene (Fc) which has a value of 4.8 eV with respect to the vacuum level.[21] The

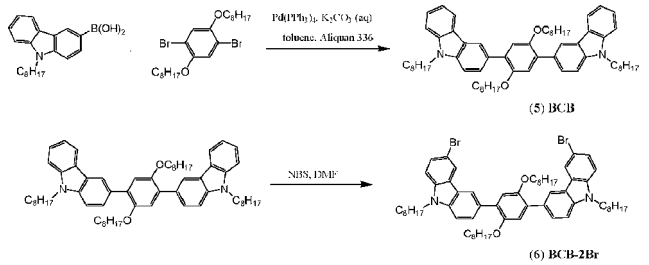

Scheme 2 Synthesis of monomer **BCB-2Br (6)**

HOMO levels of copolymers **P1–P10** (5.38–5.46 eV) were higher than that of PF (~5.77 eV)[22] because of the incorporation of **BCB** units. The energy band gaps of **P1–P10** also increased slightly compared to that of PF, which can be attributed to deconjugation of the fluorenyl segments after introduction of **BCB** units. This result showed that the introduction of **BCB** units into the polymer main chains led to a rise in HOMO levels, which implied a much lower energy barrier for the hole injection. Similar behavior was also reported for polymer P(F-*alt*-Cz) with a similar backbone.[23] The HOMO in combination with the optical band gaps derived from the absorption band edges were used to calculate the energies of the lowest unoccupied molecular orbital (LUMO) levels of the polymers. The HOMO and LUMO data are also demonstrated in Table 2.

Thermal analysis

The thermal properties of the copolymers were investigated by differential scanning calorimeter (DSC) and thermal gravimetric analysis (TGA) under nitrogen. Thermal analysis data for the copolymers and iridium monomers are also illustrated in Table 2. All copolymers (**P1–P10**) and iridium complexes (**3** and **4**) exhibited good thermal stability with thermal decomposition temperatures (T_d at 5% weight loss) ranging from 310 to 412 °C. In contrast, poly(9,9-diakylfluorene) was reported to have a thermal decomposition temperature at ~390 °C under dry nitrogen.[24] In our study, T_d was observed to decrease as the feeding ratio of iridium units increased. No obvious phase transitions of all copolymers (**P1–P10**) were detected by DSC in the temperature range of 30–300 °C.

Table 1 Molecular weight data of copolymers **P1–P10**

Copolymer	*Mn* [a]	*Mw* [a]	PDI [a]	Monomer feed ratio [b] F: BCB: Ir	Monomer composition observed [c]
P1	20500	33900	1.65	75 : 25 : 0	75.4 : 24.6 : 0
P2	5120	10700	2.08	50 : 50 : 0	48.8 : 51.2 : 0
P3	7400	14400	1.93	74 : 24 : 2	75 : 25 : 0
P4	11700	17900	1.53	72.5 : 22.5 : 5	70.2 : 25 : 4.8
P5	9630	16300	1.69	70 : 20 : 10	71.3 : 20 : 8.7
P6	8700	13600	1.56	60 : 20 : 20	65 : 22 : 13
P7	7000	11400	1.62	50 : 48 : 2	50 : 50 : 0
P8	6000	10000	1.66	50 : 45 : 5	50.3 : 45.5 : 4.2
P9	5000	10400	2.08	50 : 40 : 10	55 : 36.6 : 8.4
P10	5800	11400	1.96	50 : 30 : 20	53 : 31 : 16

[a] Molecular weights were determined by GPC using polystyrene standards. [b] The feed ratio of **F** : **BCB** : iridium complex. [c] The iridium contents (**F** : **BCB** : iridium unit) in copolymers were estimated by ^{1}H NMR.

Table 2 Electrochemical and thermal properties of Ir-complexes **3–4** and copolymers **P1–P10**

Copolymer or Ir-complex	E_{ox} [a]/V	HOMO [b]/eV	LUMO [c]/eV	E_g/eV	T_d/°C
3	0.47	5.27	2.47	2.80	363
4	0.32	5.12	2.32	2.80	322
P1	0.60	5.40	2.48	2.92	409
P2	0.58	5.38	2.28	3.10	412
P3	0.62	5.42	2.30	2.92	401
P4	0.65	5.45	2.50	2.92	334
P5	0.63	5.43	2.51	2.92	320
P6	0.62	5.44	2.51	2.93	310
P7	0.61	5.41	2.31	3.10	385
P8	0.66	5.46	2.36	3.10	365
P9	0.63	5.43	2.33	3.10	343
P10	0.64	5.45	2.33	3.10	323

[a] Oxidation potential was adjusted by using ferrocene ($E_{1/2}$ = 250 mV *vs.* $Ag/AgNO_3$) as an internal reference. Conditions of cyclic voltammetric measurements: Pt working electrode; $Ag/AgNO_3$ reference electrode. Scan rate: 100 mV s^{-1}. Electrolyte: tetrabutylammonium hexafluorophosphate. [b] HOMO levels were calculated from CV potentials using ferrocene as a standard [HOMO = 4.8 + (E_{ox} − E_{Fc})]. [c] LUMO levels were derived *via* eq. E_g = HOMO–LUMO, where E_g was obtained from the absorption spectra.

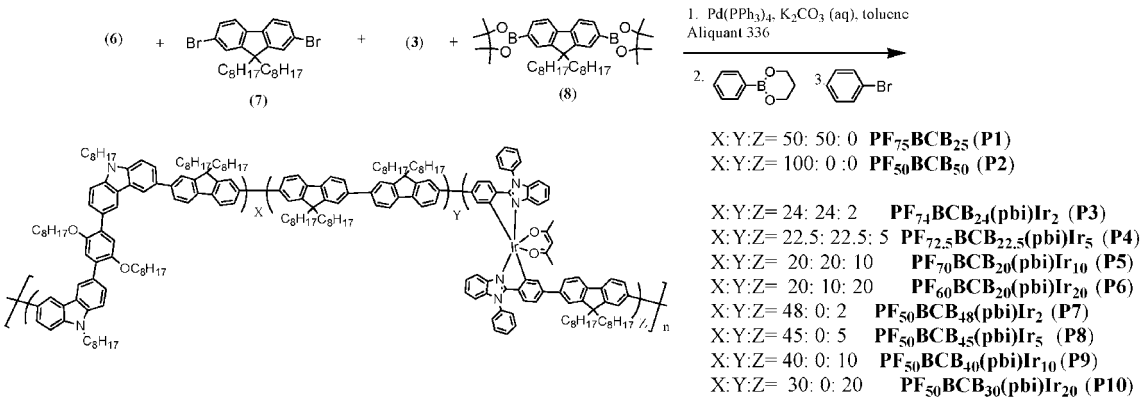

Scheme 3 Synthetic routes of copolymers **P1–P10**

Optical properties

The UV-vis absorption spectra (in CH_2Cl_2 solutions) are shown in Fig. 1 and the photophysical data are illustrated in Table 3. In Fig. 1(a), iridium complexes **3** and **4** showed strong absorption bands at 273–370 nm attributed to the π–π* transition of benzimidazolyl ligands and weak bands at 400–500 nm attributed to the ^{1}MLCT and ^{3}MLCT transitions.[19] In Fig. 1(b), the intense bands of all copolymers at ~343–382 nm can be assigned to the π–π* transition of the polymer backbones and the benzimidazole ligands. Compared with **P2** and **P7–P10**, the π–π* transition bands shifted to a shorter wavelength as the content of BCB in copolymers **P1** and **P3–P6** increased, respectively, indicating that the presence of 3,6-carbazole linkages interrupted the delocalization of π-electrons along the polymer backbones.[25] For example, due to the higher content of **BCB** units in **P2**, the absorption peak in CH_2Cl_2 solution of **P2** was blue shifted by 28 nm (371 to 343 nm) compared with that of **P1**. The weak MLCT bands at 400–500 nm were partially overlapped with the π–π* transition bands. The absorption spectra of copolymers were slightly red shifted in solid films due to the π–π stacking of molecules.

The photoluminescence (PL) properties of Ir-complexes **3** and **4**, copolymers **P1–P10**, and Ir-doped copolymers are given in Table 3. Representative PL spectra of the Ir-complexes **3** and **4** (in toluene) and selected copolymers (**P5**, **P6**, **P9**, and **P10** in dichloromethane) are shown in Fig. 2(a) and 2(b), respectively. In Fig. 2(a), it is important to note that the PL emission of Ir-complex **4** is red shifted in comparison with that of **(pbi)$_2$Ir(acac)**, which was attributed to the extension of the ligand conjugation with fluorene units in Ir-complex **4**. In Fig. 2(b), all copolymers (**P1–P10**) and Ir-doped copolymers (**P1** and **P2** with different mol% Ir-complex **4**) emitted only characteristic violet-blue light in dilute dichloromethane solutions due to the π–π* transition of the polymers as excited at 350 nm. Apparently, energy transfer from the polymer backbone to the iridium unit was very inefficient in the solution either intramolecularly or intermolecularly. Fig. 2(c) and 2(d) showed the PL spectra of Ir-copolymers **P3–P10** in solid films, and Fig. 2(e) and 2(f) were the PL spectra of Ir-doped copolymers in solid films. From **P1** to **P2**, there were blue shifts of PL spectra in both CH_2Cl_2 solutions (9 nm) and solid films (24 nm), which was consistent with the trend observed in the absorption spectra. However, phosphorescence emission of Ir-copolymers (**P3–P10**) and Ir-doped copolymers from the iridium units was more obvious in solid films, especially for higher concentration (10 and 20 mol%) of iridium units, indicating the presence of energy transfer from π–π* transitions to MLCT bands. The efficiency of the energy transfer appeared to be higher as the **BCB** ratio in the polymer backbone increased, *i.e.* **P8**, **P9**, **P10** and Ir-doped **P2** were more efficient than **P4**, **P5** and **P6**, and Ir-doped **P1**, respectively. Accordingly, the PL spectra of **P4**, **P5,** **P6** and Ir-doped **P1** exhibited more residual blue emissions. Besides the larger HOMO/LUMO gap, the larger triplet energy (E_T), and thus less energy back transfer in **P8**, **P9, P10** and Ir-doped **P2** were believed to be also the cause of their higher phosphorescence efficiencies. This argument was supported by the longer phosphorescence lifetimes of **P7–P10**, and Ir-doped **P2** than **P3–P6** and Ir-doped **P1**. The former and the latter were measured to be 0.97–1.17 μs and 0.1–0.85 μs, respectively. Compared with the relative emission intensity of phosphorescence *vs.* fluorescence in the Ir-copolymers of Fig. 2(d), the energy transfer appeared to be more efficient in the Ir-doped copolymers of Fig. 2(f). This observation implied that the intermolecular energy transfer in Ir-doped copolymers occurred more readily than the main-chain intramolecular energy transfer in Ir-copolymers. In addition, the efficiency of the energy transfer increased as the iridium content increased in both Ir-doped copolymers and Ir-copolymers.

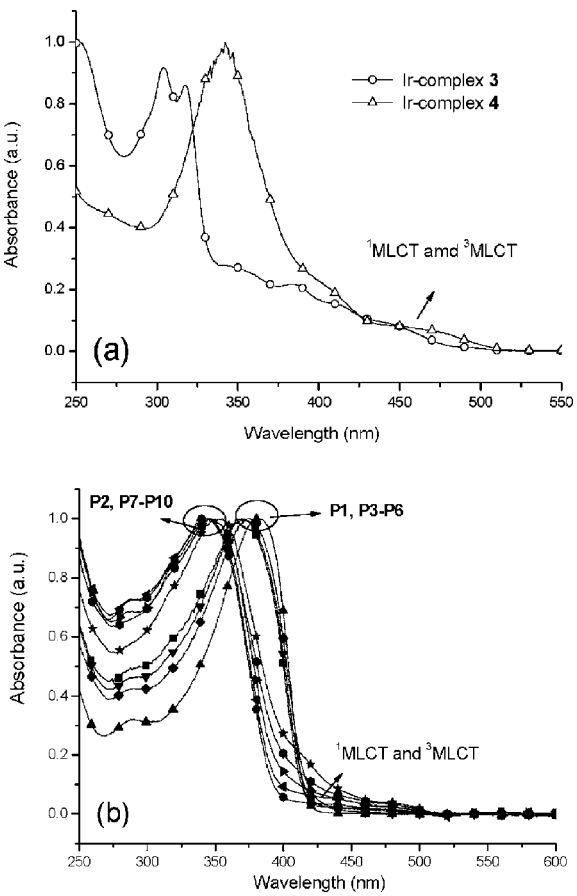

Fig. 1 UV-vis absorption spectra in CH_2Cl_2 solutions of (a) Ir-complexes **3**–**4** (b) all copolymers **P1–P10**.

The PL quantum yield (QY) values of the copolymers are also listed in Table 3. The phosphorescence QY values of Ir-complexes **3** and **4** were 30% and 25% in degassed toluene solutions, and 3.6% and 2.5% in solid films, respectively. Compared with the QY values of **P1** and **P2** in solid films (30% and 25%, respectively), Ir-copolymers **P3–P10** and Ir-doped copolymers **P1–P2** were found to have lower PL efficiencies (solid films) in the ranges of 0.3–5.5% and 1.3–8.4%, respectively.

Generally, the PL efficiencies decreased as the content of the iridium units increased. It can be rationalized by the greater tendency of triplet–triplet annihilation at higher iridium concentrations. The QY values of the Ir-copolymers and Ir-doped copolymers were higher as the **BCB** ratio in the polymer backbone increased, *i.e.*, **P8**, **P9**, **P10** and Ir-doped **P2** were higher than **P4**, **P5**, **P6** and Ir-doped **P1**, respectively. Quenching of the phosphorescence *via* energy back transfer of the phosphor excited state to the polymer triplet excited state has been well

Table 3 Photophysical properties of Ir-complexes **3–4**, copolymers **P1–P8**, and Ir-doped copolymers (**P1–P2** doped with various mol% Ir-complex **4**)

	In solution				Solid film				
	$\lambda_{max,abs}$/nm [a]	$\lambda_{PL,max}$/nm	E_T/eV	Φ_{PL} (%)	$\lambda_{max,abs}$/nm [f]	$\lambda_{PL,max}$/nm [f]	E_T/eV	Φ_{PL} (%) [h]	τ [i]
3	303, 316, 388, 416, 450	518 [b]	2.40	30 [d]		539	2.30	3.6	
4	340, 400, 452, 472	566 [b]	2.19	25 [d]		578	2.14	2.5	
P1	371	418 [a]	2.38 [c]	80 [e]	372	446	2.30 [g]	30	0.26 ns
P2	343	409 [a]	2.34 [c]	75 [e]	350	422	2.16 [g]	25	0.38 ns (75.8%)
									1.69 ns (24.2%)
P3	382	418 [a]		56 [e]	389	467		1.3	1.12 ns (47.5%)
									6.42 ns (40.4%)
									106.4 ns (12.1%)
P4	368	418 [a]		40 [e]	372	583		0.6	0.29 μs
P5	372	418 [a]		24 [e]	375	577		0.3	0.80 μs
P6	343	419 [a]		20 [e]	376	582		0.5	0.85 μs
P7	344	409 [a]		53 [e]	354	414		5.5	1.17 μs (78.7%)
									0.33 ns (21.3%)
P8	347	410 [a]		38 [e]	352	568		2.0	1.12 μs
P9	345	410 [a]		26 [e]	350	568		2.4	1.12 μs
P10	345	410 [a]		21 [e]	350	568		2.1	1.12 μs
P1 + 2 mol% **4**						565		3.8	0.82 μs
P1 + 5 mol% **4**						565		2.1	0.75 μs
P1 + 10 mol% **4**						564		2.0	0.77 μs
P1 + 20 mol% **4**						564		2.1	0.69 μs
P2 + 2 mol% **4**						563		8.4	1.07 μs
P2 + 5 mol% **4**						563		6.9	1.15 μs
P2 + 10 mol% **4**						564		5.8	1.12 μs
P2 + 20 mol% **4**						564		5.0	0.97 μs

[a] Measured in CH_2Cl_2 solutions at 298 K at a concentration of 10^{-5} M. [b] Measured in toluene solutions at 298 K. [c] Triplet energy measured at 77 K in toluene solution. [d] Quantum yields were measured with respect to $Ir(ppy)_3$ ($\Phi_{PL} = 0.4$ in toluene). The excitation wavelength was 400 nm for all Ir-complexes. [e] Measured in CH_2Cl_2 solutions in air relative to curmarin 1 ($\Phi_{PL} = 0.99$ in ethyl acetate) as a reference. The excitation wavelength was 350 nm for all copolymers. [f] Neat-film data were measured at 298 K. [g] Triplet energy measured at 77 K. [h] Neat-film data were measured at 298 K. PL quantum efficiencies in solid films were measured in an integrating sphere. The excitation wavelength was 350 nm for all copolymers. [i] Measured at 298 K. The excitation wavelength was 350 nm for all copolymers. The fluorescence lifetimes and phosphorescence lifetimes were monitored at 430 and 575 nm, respectively.

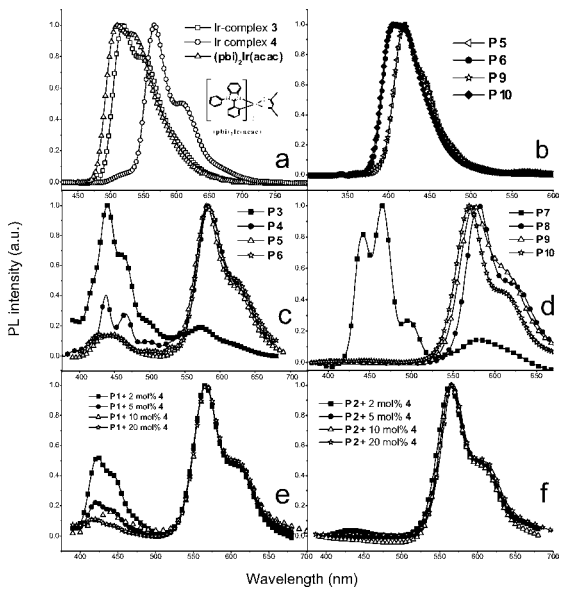

Fig. 2 PL spectra of (a) Ir-complexes **3**, **4** and **(pbi)$_2$Ir(acac)** in toluene solutions, (b) selected copolymers (**P5**, **P6**, **P9**, and **P10**) in CH_2Cl_2 solutions, (c) and (d) Ir-copolymers **P3–P8** in solid films, and (e) and (f) Ir-doped copolymers in solid films.

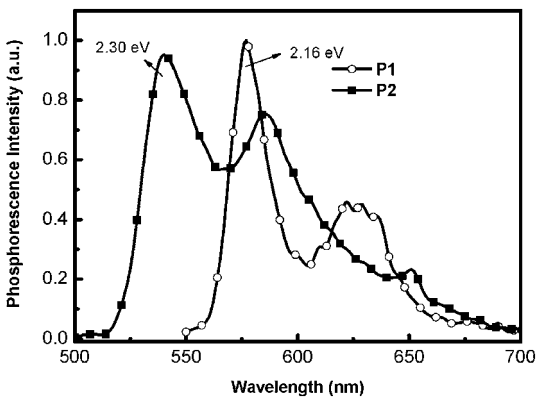

Fig. 3 Triplet energy level diagram of the **P1** and **P2** in solid films.

demonstrated for the polymer with lower triplet energy. For example, fluorene-*alt*-3,4-pyridine polymers (**PFPy**) containing iridium complexes were reported to have lower phosphorescent QY than fluorene-*alt*-thiophene polymers (**PFT**) because the lower triplet energy of **PFPy** ($E_T = 2.13$ eV) than **PFT** ($E_T = 2.88$ eV) led to more facile energy back transfer.[10b] As shown in Fig. 3, the solid film E_T of **P2** and **P1** were measured to be 2.30 and 2.16 eV, respectively, and the E_T of Ir-complex **4** was 2.14 eV (from phosphorescent emission wavelength). Fig. 4 shows a representative example illustrating the relative energy states for **P1**, **P2** and Ir-complex **4** as well as the transition between different states. It was believed that the higher film QY values of the Ir-doped copolymers (**P1** + 5, 10 and 20 mol% Ir-complex **4**) compared to the Ir-copolymers (**P4–P6**) partially benefited from

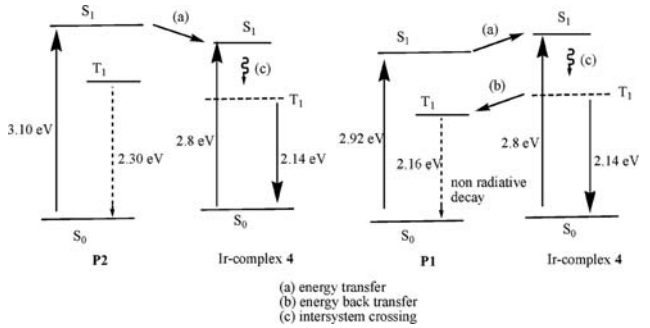

Fig. 4 Relative energy level diagram of the **P1–P2** and Ir-complex **4**.

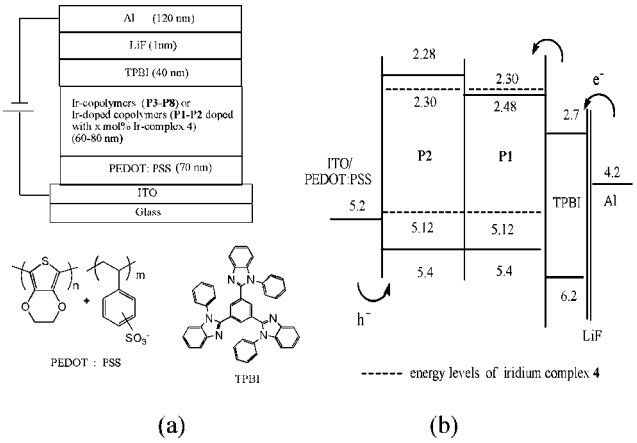

Fig. 5 (a) The configuration of PLED devices and the molecular structures of PEDOT and TPBI used in the devices and (b) relative energy levels of the compounds utilized in the PLED devices.

the less efficient energy back transfer in the former. The energy transfer efficiency depended on the distance, orientation, and overlapped area of absorption-PL spectra between the host and the guest. The slightly lower PL efficiencies of Ir-copolymers **P3–P10** may be explained by the constrained orientation of iridium complexes covalently bonded to the polymer backbones as well as the larger π–π interactions induced by the polymer main chains, which diminished the mobility of the phosphorescent iridium moieties and thus hampered the energy transfer. Therefore, less flexibilities of polymer backbones result in less efficient energy transfers in Ir-copolymers.

Electroluminescent properties

PLED devices with a configuration of ITO/PEDOT: PSS (70 nm)/Ir-copolymers (**P3–P10**) or Ir-doped copolymers (**P1–P2** doped with 2, 5, 10 or 20 mol% Ir-complex **4**) (60–80 nm)/TPBI (40 nm)/LiF (1 nm)/Al (120 nm) were fabricated, where the vacuum deposited TPBI was used as an electron-transporting and hole-blocking layer. PLED devices without TPBI were excluded due to the extremely low efficiencies (reduced by at least one order of magnitude). The configuration of PLED devices and the chemical structures of materials used in this study are shown in Fig. 5(a) and the energy levels of PLED devices are shown in Fig. 5(b). The EL spectra and the EL performance data of all PLED devices are shown in Fig. 6 and Table 4, respectively.

The EL performance parameters were in the order **P7–P10** ($\eta_{ext,max}$ = 0.89–1.53%, and $\eta_{c,max}$ = 1.55–4.14 cd A^{-1}) > **P3–P6** ($\eta_{ext,max}$ = 0.59–1.15%, and $\eta_{c,max}$ = 0.61–2.87 cd A^{-1}) and Ir-doped copolymer **P2** ($\eta_{ext,max}$ = 1.27–4.09%, and $\eta_{c,max}$ = 1.55–10.94 cd A^{-1}) > **P1** ($\eta_{ext,max}$ = 1.05–1.83%, and $\eta_{c,max}$ = 2.20–2.99 cd A^{-1}). The EL characteristic curves of current efficiency and luminance *vs.* current density of selected PLED devices are shown in Fig. 7.

Similar to the PL spectra in solid films, the EL spectra of PLED devices containing Ir-copolymers (**P3–P10**) (Fig. 6(a), and 6(b)) and Ir-doped copolymers (Fig. 6(c), and 6(d)) have both contributions from the polymer backbones and iridium moieties. However, the relative emission intensity of the iridium unit *vs.* polymer backbones in the EL spectra was different from that in the PL spectra. If the host does not have sufficiently high triplet energy, energy back transfer can occur readily, either intermolecularly[26] or intramolecularly,[27] which will counteract the contribution of phosphor molecule which has the theoretical maximum value of 75%. In addition to inefficient energy transfer

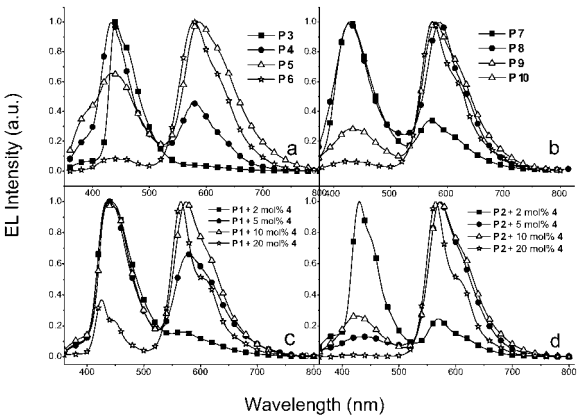

Fig. 6 EL spectra (at 10 V) of various PLED devices containing Ir-copolymers: (a) and (b), and Ir-doped copolymers: (c) and (d).

from the host to the guest, energy back transfer from the guest to the host may be also the cause of the stronger blue emission in the EL spectra than that in the PL spectra. In this study, the E_T of **P2**, **P1**, and Ir-complex **4** were 2.30, 2.16, and 2.14 eV, respectively (vide supra). Therefore, the energy back transfer from Ir-complex **4** to **P1** had a greater tendency than that from **4** to **P2** and the relative phosphorescence intensity of **4** to **P1** is smaller than that of **4** to **P2** in the PLED devices as shown in Fig. 6(c) and 6(d). Similarly, the energy back transfers of **P3–P6** (Fig. 6(a)) were more facile than those of **P7–P10** (Fig. 6(b)).

It was realized that the EL emission of the polymer backbone (with a shorter emission wavelength) increased relative to that of the iridium units (with a longer emission wavelength) as the operating voltage of PLED devices increased. Such an outcome may be attributed to the increased probability of energy back transfer because of the greater amount of triplet excitons generated at higher voltages. White light-emitting PLEDs may be possible form these materials possessing a dual emission (blue and yellow-orange) characteristic. Ir-copolymer **P8** (with 5 mol% iridium units) and Ir-doped copolymer **P2** (with 5 mol% Ir-complex **4**) were therefore tested. The EL spectra and the CIE (Commission Internationale d'Eclairage) coordinates of the two

Table 4 EL properties of PLED devices containing Ir-copolymers (**P3–P10**) and Ir-doped copolymers (**P1–P2**) doped with various mol% Ir-Complex **4**[a]

	V_{ON} V	L,max (at V) cd m^{-2}	$\eta_{ext,\ max}$ %	$\eta_{c,\ max}$ cd A^{-1}	$\lambda_{em,max}$ at 10 V nm	CIE at 10 V x,y
P3	5.0	470 (18.0)	0.59	0.61	436	0.16, 0.10
P4	4.5	1000 (18.0)	0.82	1.53	428	0.27, 0.21
P5	4.5	1040 (17.5)	1.15	2.87	580	0.40, 0.30
P6	4.0	3195 (13.5)	0.94	2.47	580	0.50, 0.44
P7	4.5	1500 (15.0)	0.89	1.55	422	0.25,0.19
P8	5.0	1960 (18.0)	0.93	1.88	576	0.35, 0.32
P9	4.0	2300 (18.0)	1.39	3.45	576	0.45, 0.38
P10	4.0	2176 (15.0)	1.53	4.14	576	0.50, 0.45
P1 + 2 mol% **4**	4.5	1810 (12.5)	1.83	2.99	414	0.31, 0.26
P1 + 5 mol% **4**	4.5	2030 (12.5)	1.62	2.66	420	0.36, 0.25
P1 + 10 mol% **4**	5.0	1980 (17.0)	1.48	2.20	434	0.28, 0.21
P1 + 20 mol% **4**	5.0	4950 (14.5)	1.05	2.84	566	0.42, 0.41
P2 + 2 mol% **4**	3.5	2710 (12.5)	1.27	1.55	430	0.23, 0.16
P2 + 5 mol% **4**	4.0	4870 (17.0)	4.09	10.94	572	0.40, 0.35
P2 + 10 mol% **4**	4.0	6150 (17.0)	3.55	8.59	574	0.45, 0.44
P2 + 20 mol% **4**	5.0	6820 (15.0)	2.18	5.87	564	0.49, 0.51

[a] V_{on}, turn-on voltage; L, luminance; V, voltage; η_{ext}, external quantum efficiency; η_c, current efficiency.

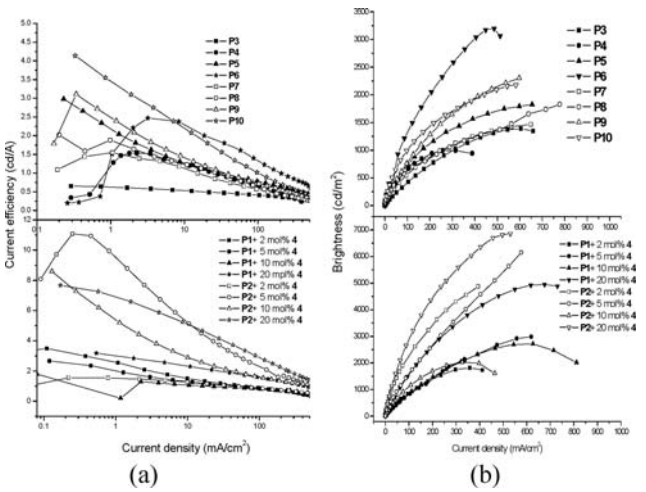

Fig. 7 The EL characteristic curves of PLED devices containing Ir-copolymers (**P3–P10**) and Ir-doped copolymers (a) current efficiency *vs.* current density plots and (b) luminance *vs.* current density plots.

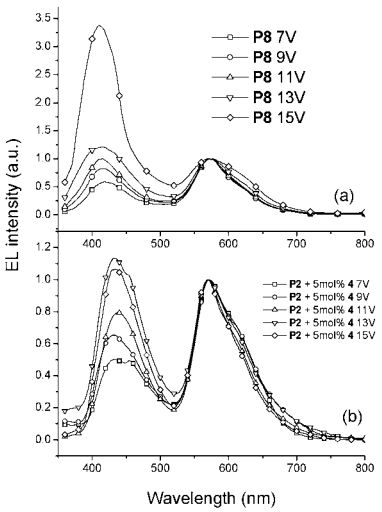

Fig. 8 EL spectra of PLED devices containing Ir-copolymers (with 5 mol% iridium units) (a) **P8** and (b) **P2** doped with 5 mol% Ir complex **4** at various voltages.

devices are shown in Fig. 8 and 9, respectively. At lower driving voltages, yellow-orange phosphorescence was prominent because of facile charge-trapping at the iridium unit. At higher driving voltages, the blue emission of the polymer backbone dominated over the phosphorescence because both singlet and triplet excitons of the polymer backbone increased significantly. The iridium phosphorescence was further suppressed at higher driving voltages because of higher concentrations of triplet excitons formed in the polymer backbones. The increased singlet excitons led to enhance the blue emission, while the increased triplet excitons suppressed the phosphorescence from the iridium units. The best EL properties of this study were found in PLED devices containing Ir-copolymers **P8** (with $\eta_{ext,max} = 0.93\%$, $\eta_{c,max} = 1.88$ cd A^{-1}, and $L_{max} = 1960$ cd m^{-2}) and **P2** doped with 5 mol% Ir-complex **4** (with $\eta_{ext,max} = 4.09\%$, $\eta_{c,max} = 10.94$ cd A^{-1}, and $L_{max} = 4870$ cd m^{-2}), respectively. The CIE coordinates, color-rendering index (CRI) and correlated color temperature (CCT) of the two PLED devices were (0.33, 0.30) at 13V, 74 and 5966 K for the former, and (0.35, 0.32) at 15 V, 82 and 6147 K for the latter, respectively.

Conclusions

In conclusion, a series of novel copolymers consisting of **BCB** segments and benzimidazole-based iridium units in the backbone by Suzuki coupling reaction were developed in this report. Incorporation of **BCB** units into the polymer backbones led to the rises in HOMO–LUMO bandgaps and the increases in triplet energy levels. As the content of **BCB** units in the copolymers increased, more efficient energy transfers were induced from the polymer backbones to the iridium units, and less efficient energy back transfers from the iridium units to the polymer backbones due to the enlarged triplet energy of the latter. Both

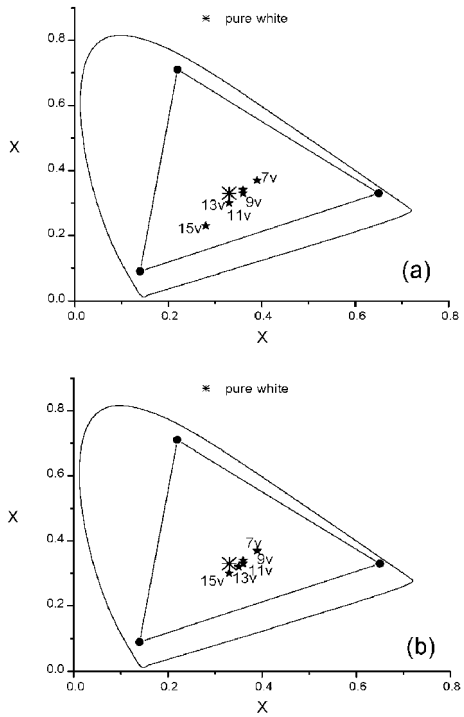

Fig. 9 CIE coordinates of various PLED devices containing (a) Ir-copolymers **P8** and (b) Ir-doped **P2** with 5 mol% Ir-complex **4** at low and high voltages (8–15 V).

Ir-copolymers (**P3–P10**) and Ir-doped copolymers (**P1–P2** with Ir-complex **4**) were used as the emitting layer of phosphorescent PLEDs. Copolymers with larger triplet energies of the polymer backbones had better performance due to more efficient suppression of energy back transfer. Less energy back transfer also led to better performance of the Ir-doped systems compared to the Ir-tethered systems. WOLED can be fairly achieved with the use of **P8** and **P2** doped with 5 mol% Ir-complex **4**. The CIE coordinates, color-rendering index (CRI) and correlated color temperature (CCT) of the two PLED devices were (0.33, 0.30) at 13V, 74 and 5966 K from the former, and (0.35, 0.32) at 15 V, 82 and 6147 K from the latter, respectively.

Experimental

General methods

^{1}H NMR spectra were recorded on a Bruker AMX400 spectrometer. FAB-mass spectra were collected on a JMS-700 double focusing mass spectrometer (JEOL, Tokyo, Japan) with a resolution of 3000 for low resolution and 8000 for high resolution (5% valley definition). The source accelerating voltage was operated at 10 kV with a Xe gun for FAB-mass spectra, using 3-nitrobenzyl alcohol as the matrix. The molecular weights of the polymers were determined by a Viscotek TriSEC GPC in THF solvent. The number-average and weight-average molecular weights were estimated by using a calibration curve of polystyrene standards. Elemental analyses were performed on a Perkin-Elmer 2400 CHN analyzer. Cyclic voltammetry (CV) experiments were performed with a CHI-621B electrochemical analyzer and carried out at room temperature with a conventional three-electrode configuration consisting of a platinum working electrode, an auxiliary electrode, and a nonaqueous $Ag/AgNO_3$ reference electrode. The solvent used in all CV experiments was CH_2Cl_2 and the supporting electrolyte was 0.1 M tetrabutylammoniumhexafluorophosphate (Bu_4NPF_6). The $E_{1/2}$ values were determined to be as $1/2(E_p^a + E_p^c)$, where E_p^a and E_p^c were the anodic and cathodic peak potentials, respectively. All reported potentials were referenced to Fc^+/Fc external standard (+0.250 V relative to the $Ag/AgNO_3$ electrode). Electronic absorption spectra were obtained on a Cary 50 Probe UV-visible spectrometer. Emission spectra were recorded in deoxygenated solutions at 298 K by a JASCO FP-6500 fluorescence spectrometer. The emission spectra in solutions were collected on samples with O.D. ~0.1 at the excitation wavelength. Emission maxima were reproducible within 2 nm. The fluorescence and phosphorescence solution quantum yields were calculated relative to coumarin 1 standard ($\Phi_{em} = 0.99$ in ethyl acetate)[28] and $Ir(ppy)_3$ ($\Phi_{em} = 0.4$ in toluene).[29] Luminescence lifetimes were determined on an Edinburgh FL920 time-correlated pulsed single-photon-counting instrument. The solid film quantum yields were measured with an integrating sphere under an excitation wavelength of 350 nm on a quartz glass. Phosphorescence spectra of the compounds (in toluene solutions and solid films) were measured by a HORIBA Jobin-Yvon FluoroMax-P spectrometer at 77 K using a 10-ms delay time between the excitation with a microsecond flash lamp and the experiment. Luminescence quantum yields were taken by the average of three separate determinations and were reproducible within 10%. Differential scanning calorimetry (DSC) measurements were carried out from 30 to 300 °C using a Perkin-Elmer 7 series thermal analyzer at a heating and cooling rate of 10 °C min^{-1}. Thermogravimetric analyses (TGA) were performed on a Perkin Elmer Pyris 1 TGA at a heating rate of 10 °C min^{-1} under nitrogen.

Device fabrication and measurement

Prepatterned ITO substrates with an effective individual device area of 3.14 mm^2 were cleaned *via* repeated ultrasonic washing with detergent, deionized water, ethanol, and oxygen plasma treatment, subsequently. A layer of poly(ethylenedioxythiophene):poly(styrene-sulfonic acid) (PEDOT:PSS) (Baytron AI4083) with a thickness of 70 nm was spin-coated on the precleaned ITO glass substrates as a hole injection layer and then baked at 100 °C in air for 1 h. After, the polymers were dissolved in chlorobenzene (concentration: 10 mg mL^{-1} for the polymers) and filtered with a 0.2 μm filter, and then a thin film of polymer was coated at a spin rate of 1800 rpm (revolution per min.). The film thickness of the polymer layer was around 40–60 nm, monitored by a surface profilometer dektak 3 (Veeco/ Sloan Instrument Inc.). Then, a layer of electron transporting 1,3,5-tris(*N*-phenylbenzimidazol-2-yl)benzene (TPBI) with a thickness of 40 nm was deposited under vacuum. Finally, a layer of LiF/Al (1 nm/ 120 nm) was thermally evaporated as a cathode in a vacuum chamber (under a pressure of less than 2.5×10^{-5} torr). *I–V* curves were measured on a Keithley 2400 Source Meter in ambient environment, and light intensities were measured with a Newport 1835 Optical Meter.

Materials

Chemicals and solvents were reagent grades and purchased from Aldrich, Acros, TCI, and Lancaster Chemical Co. Solvents were dried by standard procedures. All reactions and manipulations were carried out under N_2 with the use of standard inert atmosphere and Schlenk techniques. All column chromatography was performed by using silica gel (230–400 mesh, Macherey-Nagel GmbH & Co.) as the stationary phase in a column with a length of 25–35 cm and a diameter of 2.5 cm.

Synthesis

2.4.1. 2-(4-Bromophenyl)-1-phenyl-1*H*-benzimidazole (1, pbi-Br). *N*-Phenyl-*o*-phenylenediamine (1 eq.) and 4-bromobenzaldehyde (1 eq.) were dissolved in 50 mL of 2-methoxyethanol. The mixture was heated to reflux for 48 h under nitrogen. The volatiles were removed under vacuum and the resulting solid was extracted by dichloromethane. The organic extract was washed with brine solution, dried over anhydrous $MgSO_4$, filtered and dried. The crude product was purified by column chromatography (silica gel) using a mixture of CH_2Cl_2 and hexanes (1 : 1 by volume) as the eluent to afford the pure compound as a white solid in 60% yield. ^{1}H NMR ($CDCl_3$, 400 MHz, ppm): δ 7.68 (d, J = 8.0 Hz, 1H), 7.35–7.29 (m, 4H), 7.24–7.20 (m, 1H), 7.15–7.02 (m, 7H). FABMS: m/z 348.9 $(M)^+$. Anal. calcd. for $C_{19}H_{13}BrN_2$: C, 65.35; H, 3.75; N, 8.02. Found: C, 65.22; H, 3.78; N, 8.01

2-(4-(9,9-Dihexyl-9*H*-fluoren-2-yl)phenyl)-1-phenyl-1*H*- benzimidazole (2 or pbiF). To a mixture of toluene and aqueous solution of K_2CO_3 (1 : 1 v/v, 40 mL), compound **1** (1.39 g, 4 mmol) and 2-(4,4,5,5-tetramethyl-1,3,2-dioxaborolan-2-yl)-9,9-dihexylfluorene (1.73 g, 4 mmol), and tetrakis-(triphenylphosphine)palladium ($Pd(PPh_3)_4$) (100 mg, 0.04 mmol) were added to reflux for 24 h. After cooling, the reaction was quenched with water and the mixture was extracted with dicholormethane. The combined extracts were then washed with brine, dried over $MgSO_4$, and evaporated to dryness. The crude product was isolated by column chromatography on a silica gel column using a mixture of CH_2Cl_2 and hexanes (1 : 4 by volume) as the eluent to afford the pure compound as a bright yellow powder in 40% yield. ^{1}H NMR ($CDCl_3$, 400 MHz, ppm): δ 8.19 (s, 1H), 7.92 (d, J = 8.0 Hz, 1H), 7.74 (d, J = 8.0 Hz, 2H), 7.70 (d, J = 8.4 Hz, 2H), 7.62 (d, J = 8.4 Hz, 2 H), 7.58–7.53 (m, 4H), 7.41∼7.27 (m, 8H), 2.01–1.97 (m, 4H), 1.13–1.03 (m, 12H), 0.75 (t, J = 7.5 Hz, 6H), 0.66–0.63 (m, 4H). FABMS: m/z 603.2 $(M + H)^+$ Anal. calcd. for $C_{44}H_{46}N_2$: C, 87.66; H, 7.69; N, 4.65. Found: C, 87.42; H, 7.78; N, 4.41.

(pbi-Br)$_2$Ir(acac) (3). To a flask containing $IrCl_3 \cdot nH_2O$ (176 mg, 0.5 mmol) and compound **1** (700 mg, 2.0 equiv), a mixture of 2-ethoxyethanol and water (3 : 1 v/v, 25 mL) was added. The mixture was then refluxed for 48 h and cooled to room temperature. After cooling, the reaction was quenched with water, extracted with dicholormethane, and dried under vacuum. The solid formed was collected by filtration and evaporation to give the crude product. The crude product of μ-chloro-bridged Ir(III) dimer was mixed with Na_2CO_3 (0.30 g, 3.0 mmol), 2,4-pentanedione (0.30 g, 3.0 mmol), and 2-methoxyethanol (20 mL) in a flask. The mixture was heated to reflux for 24 h. After cooling, the reaction was quenched with water and the mixture was extracted with dicholormethane. The combined extracts were then washed with brine, dried over $MgSO_4$, and evaporated to dryness. The crude product was isolated by column chromatography on a silica gel column using a mixture of CH_2Cl_2 and hexanes (1 : 1 by volume) as the eluent to afford the pure compound as a yellow solid in 65% yield. ^{1}H NMR ($CDCl_3$, 400 MHz, ppm): δ 7.68−7.63 (m, 8H), 7.60−7.58 (m, 4H), 7.32−7.27 (m, 4H), 7.14−7.11 (m, 2H), 6.64 (dd, J = 8.0 Hz and J = 2.0 Hz, 2H), 6.49 (d, J = 2.0 Hz, 2H), 6.38 (d, J = 8.4 Hz, 2H), 5.25 (s, 1H), 1.84 (s, 6H). FABMS: m/z 986.0 $(M)^+$. Anal. calcd. for $C_{43}H_{31}Br_2IrN_4O_2$: C, 52.29; H, 3.16; N, 5.67. Found: C, 52.55; H, 3.26; N, 5.56.

(pbiF)$_2$Ir(acac) (4). Compound **4** was synthesized by the same procedure as illustrated for compound **3** except that compound **1** was used instead of compound **2**. The product was isolated as an orange solid in 40% yield. ^{1}H NMR ($CDCl_3$, 400 MHz, ppm): δ 7.87 (s, 2H), 7.88 (dd, J = 7.2 Hz and 1.6 Hz, 2H), 7.69–7.55 (m, 10H), 7.50–7.48 (m, 2H), 7.46 (d, J = 8.0 Hz, 2H), 7.37–7.34 (m, 4H), 7.24–7.15 (m, 8H), 7.01 (s, 2H), 6.82 (s, 2H), 6.80 (dd, J = 8.0 Hz and 1.6 Hz, 2H), 6.60 (d, J = 8.0 Hz, 2H), 5.29 (s, 1H), 1.91 (s, 6H), 1.90–1.58 (m, 8H), 1.13–1.03 (m, 24H), 0.75 (t, J = 7.6 Hz, 12H), 0.66–0.63 (m, 8H). FABMS: m/z 1495.1 $(M)^+$. Anal. calcd. for $C_{93}H_{97}IrN_4O_2$: C, 74.71; H, 6.54; N, 3.75. Found: C, 74.44; H, 6.38; N, 3.62.

1,4-Bis(9-octyl-9*H*-carbarzol-3yl)-2,5-dioctyloxy-benzene (5 or BCB). To a mixture of toluene and aqueous solution of K_2CO_3 (1 : 1 v/v, 40 mL), 1,4-dibromo-2,5-bis(octyloxy)benzene (4.92 g, 10 mmol), 9-octyl-9*H*-carbazol-3-ylboronic acid (3.23 g, 10 mmol), and tetrakis(triphenylphosphine)palladium (120 mg) were added to reflux for 24 h. After cooling, the reaction was quenched with water and the mixture was extracted with dicholormethane. The combined extracts were then washed with brine, dried over $MgSO_4$, and evaporated to dryness. The crude product was isolated by column chromatography on a silica gel column using a mixture of CH_2Cl_2 and hexanes (1 : 20 by volume) as the eluent. The compound **5** was obtained as a pale yellow oil in 75% yield. ^{1}H NMR ($CDCl_3$, 400 MHz, ppm): δ 8.36 (s, 2H), 8.11 (d, J = 8.0 Hz, 2H), 7.75 (d, J = 8.0 Hz, 2H), 7.47–7.39 (m, 6H), 7.24–7.19 (m, 2H), 7.15 (s, 2H), 4.31 (t, J = 7.2 Hz, 4H), 3.96 (t, J = 6.4 Hz, 4H), 1.92–1.88 (m, 4H), 1.70–1.66 (m, 4H), 1.41–1.16 (m, 40H), 0.86 (t, J = 7.2 Hz, 6H), 0.80 (t, J = 6.8 Hz, 6H). FABMS: m/z 889.4 $(M)^+$.

1,4-Bis(6-bromo-9-octyl-9*H*-carbarzol-3yl)-2,5-dioctyloxy-benzene (6 or BCB-2Br). Compound **5** (7.3 g, 8.2 mmol) was dissolved in 20 mL of dimethylformamide in a 250 mL one-necked flask. *N*-Bromosuccinimide (NBS) (3.06 g, 17.2 mmol) was dissolved in 20 mL of dimethylformamide and added into the reaction flask through a dropping funnel over a period of 30 min. The mixture was stirred at room temperature for 12 h. The reaction was quenched with water and extracted with dicholormethane. The combined extract was then washed with brine, dried over $MgSO_4$, and evaporated to dryness. The crude product was isolated by column chromatography on a silica gel column using a mixture of CH_2Cl_2 and hexanes (1 : 20 by volume) as the

eluent. Compound **6** was isolated as a white solid in 80% yield. ^{1}H NMR ($CDCl_3$, 400 MHz, ppm): δ 8.29 (d, J = 1.5 Hz, 2H), 8.20 (d, J = 1.8 Hz, 2H), 7.77 (dd, J = 8.4 and J = 1.5 Hz, 2H), 7.53 (dd, J = 8.7 and 1.8 Hz, 2H), 7.43 (d, J = 8.4 Hz, 2H), 7.28 (d, J = 8.7 Hz, 2H), 7.12 (s, 2H), 4.28 (t, J = 7.2 Hz, 4H), 3.97 (t, J = 6.3 Hz, 4H), 1.89–1.81 (m, 4H), 1.73–1.64 (m, 4H), 1.41–1.16 (m, 40H), 0.85 (t, J = 7.2 Hz, 6H), 0.79 (t, J = 6.8 Hz, 6H). FABMS: m/z 1044.4 $(M)^+$.

General procedure for copolymerization by the Suzuki cross-coupling method

The following generalized procedure was used for the preparation of all copolymers. To a 50 mL, two-necked flask charged with a condenser, tricaprylymethylammonium chloride (Aliquat 336) (~20 wt% based on the monomer), diboronate (compound **8**, 1 equiv.), dibromide (compounds **3**, **6**, and **7**, 1 equiv.), and $Pd(PPh_3)_4$ (25 mg, 0.005 equiv) were added. After the flask was evacuated and refilled with nitrogen for three times, toluene (1 mL) was added. Once all monomers were dissolved, an aqueous solution of K_2CO_3 (2 M, 1 mL) was added. The mixture was heated to 100 °C and stirred for 48 h under nitrogen. Phenylboronic acid (100 mg) was added and stirred at the same temperature for 12 h. Then, bromobenzene (0.5 mL) was added in the solution and heated for another 12 h. The mixture was cooled and poured into a mixture of methanol and water (100 mL, 2 : 1 v/v). The crude copolymer was filtered, washed with excess methanol, acetone, hexanes, and dried. The polymer was dissolved in CH_2Cl_2 and precipitated with methanol for two times. The product was further purified by flash chromatography using silica gel and a mixture of dichloromethane and THF (4 : 1) as the eluent. A general nomenclatures for the copolymers (**P1–P10**) with respect to the abbreviations of their monomers and their mol% were adopted. For example, **$PF_{74}BCB_{24}(pbi)Ir_2$** (**P3**) was synthesized from the composition of the following monomers: 2 mol% dibromo-substituted Ir-complex (**3**), 24 mol% **BCB-2Br** (**6**), and 74 mol% fluorenes (**7** and **8**, abbreviated as **F**).

$PF_{75}BCB_{25}$ (P1). Following the general polymerization procedure, compound **6** (1.0 equiv), 2,7-dibromo-9,9-dioctyl-9*H*-fluorene (compound **7**, 1.0 equiv) and 2,2′-(9,9-di-n-octyl-9*H*-fluorene-2,7-diyl)*bis*(4,4,5,5,-tetramethyl)-1,3,2-dioxaborolane (compound **8**, 2.0 equiv) were used in this polymerization to acquire a bright green solid. Yield = 75%. ^{1}H NMR ($CDCl_3$, 400 MHz, ppm): δ 8.45–8.42 (d, carbazole ring), 7.85–7.78 (m, fluorene and carbazole ring), 7.72–7.65 (m, fluorene and carbazole ring), 7.50–7.40 (m, fluorene ring), 7.19 (s, -C_6H_2-), 4.39–4.31(m, N–CH_2), 4.00–3.95 (m, O–CH_2), 2.19–2.05 (fluorene-CH_2), 2.01–1.94 (m, –C_8H_{17}), 1.70–1.53 (m, –C_8H_{17}), 1.46–1.10 (m, –C_8H_{17}), 0.86–0.60 (m, –C_8H_{17}). Anal. calcd. for $(C_{29}H_{40})_{75}(C_{62}H_{82}N_2O_2)_{25}$: C, 87.16; H, 9.92; N, 1.36. Found: C, 86.86; H, 9.82; N, 1.24. GPC: M_w (weight-average molecular weight) = 33900 Da, DPI = 1.65.

$PF_{50}BCB_{50}$ (P2). Following the general polymerization procedure, compound **6** (1.0 equiv) and compound **8** (1.0 equiv) were used in this polymerization to acquire a gray solid. Yield = 78%. ^{1}H NMR ($CDCl_3$, 400 MHz, ppm): δ 8.45–8.42 (d, carbazole ring), 7.85–7.78 (m, fluorene and carbazole ring), 7.72–7.65 (m, fluorene and carbazole ring), 7.50–7.40 (m, fluorene ring), 7.19 (s, -C_6H_2-), 4.39–4.31 (m, N–CH_2), 4.00–3.95 (m, O–CH_2), 2.19–2.05 (fluorene-CH_2), 2.01–1.94 (m, –C_8H_{17}), 1.70–1.53 (m, –C_8H_{17}), 1.46–1.10 (m, –C_8H_{17}), 0.86–0.60 (m, –C_8H_{17}). Anal. calcd. for $(C_{29}H_{40})_{50}(C_{62}H_{82}N_2O_2)_{50}$: C, 85.66; H, 9.64; N, 2.20. Found: C, 84.32; H, 9.32; N, 2.24. GPC: M_w = 10700 Da, DPI = 2.08.

$PF_{74}BCB_{24}(pbi)Ir_2$ (P3). Following the general polymerization procedure, compound **3** (1.0 equiv), compound **6** (12.0 equiv), compound **7** (12.0 equiv), and compound **8** (25.0 equiv) were used in this polymerization to acquire a yellow-green solid. Yield = 72%. Anal. calcd. for $(C_{29}H_{40})_{74}(C_{62}H_{82}N_2O_2)_{24}$-$(C_{43}H_{31}IrN_4O_2)_2$: C, 86.40; H, 9.73; N, 1.52. Found: C, 85.44; H, 9.32; N, 1.43. GPC: M_w = 14400 Da, DPI = 1.93.

$PF_{72.5}BCB_{22.5}(pbi)Ir_5$ (P4). Following the general polymerization procedure, compound **3** (5.0 equiv), compound **6** (22.5 equiv), compound **7** (22.5 equiv), and compound **8** (50.0 equiv) were used in this polymerization to acquire a yellow solid. Yield = 75%. Anal. calcd. for $(C_{29}H_{40})_{72.5}(C_{62}H_{82}N_2O_2)_{22.5}$-$(C_{43}H_{31}IrN_4O_2)_5$: C, 85.29; H, 9.45; N, 1.74. Found: C, 84.82; H, 9.22; N, 1.44. GPC: M_w = 17900 Da, DPI = 1.53.

$PF_{70}BCB_{20}(pbi)Ir_{10}$ (P5). Following the general polymerization procedure, compound **3** (1.0 equiv), compound **6** (2.0 equiv), compound **7** (2.0 equiv), and compound **8** (5.0 equiv) were used in this polymerization to acquire a yellow solid. Yield = 72%. ^{1}H NMR ($CDCl_3$, 400 MHz, ppm): δ 8.45–8.42 (d, carbazole ring), 7.80–7.65 (m, fluorene and carbazole ring), 7.54–7.38 (m, fluorene ring), 7.19–7.16 (m, –C_6H_2-), 7.04–7.03 (m, benzimidazole ring), 6.75–6.70 (m, benzimidazole ring), 6.44–6.43 (m, benzimidazole ring), 4.39–4.31(m, N–CH_2), 4.00–3.95 (m, O–CH_2), 2.19–2.05 (fluorene-CH_2), 2.01–1.94 (m, –C_8H_{17}), 1.70–1.53 (m, –C_8H_{17}), 1.46–1.10 (m, –C_8H_{17}), 0.86–0.60 (m, –C_8H_{17}). Anal. calcd. for $(C_{29}H_{40})_{70}(C_{62}H_{82}N_2O_2)_{20}(C_{43}H_{31}IrN_4O_2)_{10}$: C, 83.49; H, 8.99; N, 2.11. Found: C, 82.87; H, 9.12; N, 2.20. GPC: M_w = 16300 Da, DPI = 1.69.

$PF_{60}BCB_{20}(pbi)Ir_{20}$ (P6). Following the general polymerization procedure, compound **3** (2.0 equiv), compound **6** (2.0 equiv), compound **7** (1.0 equiv), and compound **8** (5.0 equiv) were used in this polymerization to acquire an orange solid. Yield = 72%. ^{1}H NMR ($CDCl_3$, 400 MHz, ppm): δ 8.45–8.42 (d, carbazole ring), 7.80–7.65 (m, fluorene and carbazole ring), 7.54–7.38 (m, fluorene ring), 7.19–7.16 (m, –C_6H_2-), 7.04–7.03 (m, benzimidazole ring), 6.75–6.70 (m, benzimidazole ring), 6.44–6.43 (m, benzimidazole ring), 4.39–4.31(m, N–CH_2), 4.00–3.95 (m, O–CH_2), 2.19–2.05 (fluorene-CH_2), 2.01–1.94 (m, –C_8H_{17}), 1.70–1.53 (m, –C_8H_{17}), 1.46–1.10 (m, –C_8H_{17}), 0.86–0.60 (m, –C_8H_{17}). Anal. calcd. for $(C_{29}H_{40})_{60}(C_{62}H_{82}N_2O_2)_{20}(C_{43}H_{31}IrN_4O_2)_{20}$: C, 80.04; H, 8.15; N, 2.92. Found: C, 78.24; H, 9.75; N, 2.42. GPC: M_w = 13600 Da, DPI = 1.56.

$PF_{50}BCB_{48}(pbi)Ir_2$ (P7). Following the general polymerization procedure, compound **3** (1.0 equiv), compound **6** (24.0 equiv), and compound **8** (25.0 equiv) were used in this polymerization to acquire the product as a yellow solid. Yield = 85%. Anal. calcd.

for $(C_{29}H_{40})_{50}(C_{62}H_{82}N_2O_2)_{48}(C_{43}H_{31}IrN_4O_2)_2$: C, 85.10; H, 9.49; N, 2.29. Found: C, 84.41; H, 9.24; N, 1.79. GPC: M_w = 11400 Da, DPI = 1.62.

$PF_{50}BCB_{45}(pbi)Ir_5$ (P8). Following the general polymerization procedure, compound **3** (1.0 equiv), compound **6** (9.0 equiv), and compound **8** (25.0 equiv) were used in this polymerization to acquire a yellow solid. Yield = 76%. Anal. calcd. for $(C_{29}H_{40})_{50}(C_{62}H_{82}N_2O_2)_{45}(C_{43}H_{31}IrN_4O_2)_5$: C, 84.26; H, 9.28; N, 2.43. Found: C, 84.41; H, 9.24; N, 2.39. GPC: M_w = 10000 Da, DPI = 1.66.

$PF_{50}BCB_{40}(pbi)Ir_{10}$ (P9). Following the general polymerization procedure, compound **3** (1.0 equiv), compound **6** (4.0 equiv), and compound **8** (5.0 equiv) were used in this polymerization to acquire a brown solid. Yield = 54%. ^{1}H NMR ($CDCl_3$, 400 MHz, ppm): δ 8.45–8.42 (d, carbazole ring), 7.80–7.65 (m, fluorene or carbazole ring), 7.54–7.38 (m, fluorene ring), 7.19–7.16 (m, $-C_6H_2-$), 7.04–7.03 (m, benzimidazole ring), 6.75–6.70 (m, benzimidazole ring), 6.44–6.43 (m, benzimidazole ring), 4.39–4.31 (m, N–CH_2), 4.00–3.95 (m, O–CH_2), 2.19–2.05 (fluorene-CH_2), 2.01–1.94 (m, $-C_8H_{17}$), 1.70–1.53 (m, $-C_8H_{17}$), 1.46–1.10 (m, $-C_8H_{17}$), 0.86–0.60 (m, $-C_8H_{17}$). Anal. calcd. for $(C_{29}H_{40})_{50}(C_{62}H_{82}N_2O_2)_{40}(C_{43}H_{31}IrN_4O_2)_{10}$: C, 82.85; H, 8.91; N, 2.66. Found: C, 82.41; H, 8.64; N, 2.38. GPC: M_w = 10400 Da, DPI of 2.08.

$PF_{50}BCB_{30}(pbi)Ir_{20}$ (P10). Following the general polymerization procedure, compound **3** (2.0 equiv), compound **6** (3.0 equiv), and compound **8** (5.0 equiv) were used in this polymerization to acquire a brown solid. Yield = 54%. ^{1}H NMR ($CDCl_3$, 400 MHz, ppm): δ 8.45–8.42 (d, carbazole ring), 7.80–7.65 (m, fluorene or carbazole ring), 7.54–7.38 (m, fluorene ring), 7.19–7.16 (m, $-C_6H_2-$), 7.04–7.03 (m, benzimidazole ring), 6.75–6.70 (m, benzimidazole ring), 6.44–6.43 (m, benzimidazole ring), 4.39–4.31 (m, N–CH_2), 4.00–3.95 (m, O–CH_2), 2.19–2.05 (fluorene-CH_2), 2.01–1.94 (m, $-C_8H_{17}$), 1.70–1.53 (m, $-C_8H_{17}$), 1.46–1.10 (m, $-C_8H_{17}$), 0.86~0.60 (m, $-C_8H_{17}$). Anal. calcd. for $(C_{29}H_{40})_{50}(C_{62}H_{82}N_2O_2)_{30}(C_{43}H_{31}IrN_4O_2)_{20}$: C, 79.99 H, 8.18; N, 3.13. Found: C, 77.41; H, 7.14; N, 2.88. GPC: M_w = 11400 Da, DPI of 1.96.

Acknowledgements

The authors express their sincere thanks to the Academia Sinica, National Chiao Tung University, and the National Science Council for supporting this work.

Notes and references

1 C. W. Tang and S. A. Van Slyke, *Appl. Phys. Lett.*, 1987, **51**, 913.
2 J. H. Burroughes, D. D. C. Bradley, A. R. Brown, R. N. Marks, K. Mackay, R. H. Friend, P. L. Burn and A. B. Holmes, *Nature*, 1990, **347**, 539.
3 (*a*) M. A. Baldo, D. F. O'Brien, Y. You, A. Shoustikov, S. Sibley, M. E. Thompson and S. R. Forrest, *Nature*, 1998, **395**, 151; (*b*) M. A. Baldo, D. F. O'Brien, M. E. Thompson and S. R. Forrest, *Phys. Rev. B: Condens. Matter Mater. Phys.*, 1999, **60**, 14422.
4 (*a*) H. Z. Xie, M. W. Liu, O. Y. Wang, X. H. Zhang, C. S. Lee, L. S. Hung, S. T. Lee, P. F. Teng, H. L. Kwong, H. Zheng and C. Che, *Adv. Mater.*, 2001, **13**, 1245; (*b*) V. V. Grushin, N. Herron, D. D. LeCloux, W. J. Marshall, V. A. Petrov and Y. Wang, *Chem. Commun.*, 2001, 1494; (*c*) J. Ostrowski, M. R. Robinson, A. J. Heeger and G. C. Bazan, *Chem. Commun.*, 2002, 784; (*d*) J.-P. Duan, P.-P. Sun and C.-H. Cheng, *Adv. Mater.*, 2003, **15**, 224; (*e*) Y.-J. Su, H.-L. Huang, C.-L. Li, C.-H. Chien, Y.-T. Tao, P.-T. Chou, S. Datta and R.-S. Liu, *Adv. Mater.*, 2003, **15**, 884; (*f*) A. B. Tamayo, B. D. Alleyne, P. I. Djurovich, S. Lamansky, I. Tsyba, N. N. Ho, R. Bau and M. E. Thompson, *J. Am. Chem. Soc.*, 2003, **125**, 7377.
5 (*a*) W. Lu, B.-X. Mi, M. C. W. Chan, Z. Hui, N. Zhu, S.-T. Lee and C.-M. Che, *Chem. Commun.*, 2002, 206; (*b*) B. W. D'Andrade, J. Brooks, V. Adamovich, M. E. Thompson and S. R. Forrest, *Adv. Mater.*, 2002, **14**, 1032.
6 (*a*) Y. Ma, H. Zhang, J. Shen and C.-M. Che, *Synth. Met.*, 1998, **94**, 245; (*b*) J. Lu, Y. Tao, Y. Chi and Y.-Y. Tung, *Synth. Met.*, 2005, **155**, 56; (*c*) Y.-H. Niu, Y.-L. Tung, Y. Chi, C.-F. Shu, J. H. Kim, B. Chen, J. Luo, A. J. Carty and A. K.-Y. Jen, *Chem. Mater.*, 2005, **17**, 3532; (*d*) C.-H. Chien, P.-I. Shih, F.-I. Wu, C. F. Shu and Y. Chi, *J. Polym. Sci., Part A: Polym. Chem.*, 2007, **45**, 2073.
7 (*a*) H. Xia, C. Zhang, X. Liu, S. Qiu, P. Lu, F. Shen, J. Zhang and Y. Ma, *J. Phys. Chem. B*, 2004, **108**, 3185; (*b*) F. G. Gao and A. J. Bard, *J. Am. Chem. Soc.*, 2000, **122**, 7426.
8 (*a*) Y. Y. Chen, Y. T. Tao and H. C. Lin, *Macromolecules*, 2006, **39**, 8559; (*b*) Y. Y. Chen and H. C. Lin, *Polymer*, 2007, **48**, 5268; (*c*) Y. Y. Chen and H. C. Lin, *J. Polym. Sci., Part A: Polym. Chem.*, 2007, **45**, 3243; (*d*) K. L. Paik, N. S. Baek and H. K. Kim, *Macromolecules*, 2002, **35**, 6782; (*e*) X. Gong, D. Moses, A. J. Heeger and S. Xiao, *J. Phys. Chem. B*, 2004, **108**, 8601; (*f*) S.-C. Lo, G. J. Richard, J. P. J. Markham, E. B. Namdas, S. Sharma, P. L. Burn and I. D. W. Samuel, *Adv. Funct. Mater.*, 2005, **15**, 1451; (*g*) S.-C. Lo, N. A. H. Male, J. P. J. Markham, S. W. Magennis, P. L. Burn and I. D. W. Samuel, *Adv. Mater.*, 2002, **14**, 975.
9 (*a*) B. W. D. Andrade, M. E. Thompson and S. R. Forrest, *Adv. Mater.*, 2002, **14**, 147; (*b*) J. Feng, F. Li, W. Gao, S. Liu, Y. Liu and Y. Wang, *Appl. Phys. Lett.*, 2001, **78**, 3947.
10 (*a*) J. R. Carlise, X. Y. Wang and M. Weck, *Macromolecules*, 2005, **38**, 9000; (*b*) C. L. Schulz, X. Chen, S.-A. Chen and S. Holdcroft, *Macromolecules*, 2006, **39**, 9157; (*c*) N. R. Evans, L. S. Devi, C. S. K. Mak, S. E. Watkins, S. I. Pascu, A. Köhler, R. H. Friend, C. K. Willans and A. B. Holms, *J. Am. Chem. Soc.*, 2006, **128**, 6647.
11 (*a*) X. Gong, M. R. Robinson, J. C. Ostrowski, D. Moses, G. C. Bazan and A. J. Hegger, *Adv. Mater.*, 2002, **14**, 581; (*b*) Y. Kawamura, S. Yanagida and S. R. Forrest, *J. Appl. Phys.*, 2002, **92**, 87; (*c*) K.-M. Yeh, C.-C. Lee and Y. Chen, *J. Polym. Sci., Part A: Polym. Chem.*, 2008, **46**, 5180; (*d*) C.-F. Liao, B.-Y. Hsieh and Y. Chen, *J. Polym. Sci., Part A: Polym. Chem.*, 2009, **47**, 149.
12 (*a*) H. Zhen, C. Luo, W. Yang, W. Song, B. Du, J. Jiang, C. Jiang, Y. Zhang and Y. Cao, *Macromolecules*, 2006, **39**, 1693; (*b*) K. Zhang, Z. Chen, Y. Zou, C. Yang, J. Qin and Y. Cao, *Organometallics*, 2007, **26**, 3699.
13 (*a*) X. W. Chen, J. L. Liao, Y. M. Liang, M. O. Ahmed, H. E. Tseng and S.-A. Chen, *J. Am. Chem. Soc.*, 2003, **125**, 636; (*b*) J. Jiang, C. Jiang, W. Yang, H. Zhen, F. Huang and Y. Cao, *Macromolecules*, 2005, **38**, 4072.
14 (*a*) P.-I. Lee and S. L.-C. Hsu, *J. Polym. Sci., Part A: Polym. Chem.*, 2007, **45**, 1492; (*b*) K. Zhang, Z. Chen, C. Yang, Y. Zou, S. Gong, Y. Tao, J. Qin and Y. Cao, *J. Mater. Chem.*, 2008, **18**, 3366.
15 (*a*) Q. Pei and Y. Yang, *J. Am. Chem. Soc.*, 1996, **118**, 7416; (*b*) J. Jacob, J. Zhang, A. C. Grimsdale, K. Müllen, M. Gaal and E. J. W. List, *Macromolecules*, 2003, **36**, 8240; (*c*) H.-J. Cho, B.-J. Jung, N. S. Cho, J. Lee and H.-K. Shim, *Macromolecules*, 2003, **36**, 6704; (*d*) B. J. Jung, J.-I. Lee, H. Y. Chu, L.-M. Do and H.-K. Shim, *Macromolecules*, 2002, **35**, 2282.
16 J. X. Jiang, Y. H. Xu, W. Yang, R. Guan, Z. Q. Lin, H. Y. Zhen and Y. Cao, *Adv. Mater.*, 2006, **18**, 1769.
17 F.-I. Wu, X.-H. Yang, D. Neher, R. Dodda, Y.-H. Tseng and C. F. Shu, *Adv. Funct. Mater.*, 2007, **17**, 1085.
18 P.-I. Lee, S. L.-C. Hsu and J.-F. Lee, *J. Polym. Sci., Part A: Polym. Chem.*, 2008, **46**, 464.
19 W.-S. Huang, J. T. Lin, C.-H. Chien, Y.-T. Tao, S.-S. Sun and Y.-S. Wen, *Chem. Mater.*, 2004, **16**, 2480.
20 (*a*) W.-S. Huang, J. T. Lin and H.-C. Lin, *Org. Electron.*, 2008, **9**, 557; (*b*) W.-S. Huang, C.-W. Lin, J. T. Lin, J.-H. Huang, C.-W. Chu, Y.-S. Wu and H.-C. Lin, *Org. Electron.*, 2009, **10**, 594.

21 J. Pommerehne, H. Vestweber, W. Guss, R. F. Mahrt, H. Bässler, M. Porsch and J. Daub, *Adv. Mater.*, 1995, **7**, 551.
22 H. Y. Zhen, C. Y. Jiang, W. Yang, J. X. Jiang, F. Huang and Y. Cao, *Chem.–Eur. J.*, 2005, **11**, 5007.
23 Y. Li, J. F. Ding, M. Day, Y. Tao, J. P. Lu and M. D'iorio, *Chem. Mater.*, 2004, **16**, 2165.
24 B. Liu, W.-L. Yu, Y.-H. Lai and W. Huang, *Chem. Mater.*, 2001, **13**, 1984.
25 C. Xia and R. C. Advincula, *Macromolecules*, 2001, **34**, 5854.
26 (*a*) C. Adachi, R. C. Kwong, P. Djurovich, V. Adamovich, M. A. Baldo, M. E. Thompson and S. R. Forrest, *Appl. Phys. Lett.*, 2001, **79**, 2082; (*b*) M. Sudhakar, P. I. Djurovich, T. E. Hogen-Esch and M. E. Thompson, *J. Am. Chem. Soc.*, 2003, **125**, 7796.
27 Y. You, S. H. Kim, H. K. Jung and S. Y. Park, *Macromolecules*, 2006, **39**, 349.
28 G. Jones II, W. R. Jackson, C. Y. Choi and W. R. Bwrgmark, *J. Phys. Chem.*, 1985, **89**, 294.
29 A. Tsuboyama, H. Iwawaki, M. Furugori, T. Mukaide, J. Kamatani, S. Igawa, T. Moriyama, S. Miura, T. Takiguchi, S. Okada, M. Hoshino and K. Ueno, *J. Am. Chem. Soc.*, 2003, **125**, 12971.